# Chaotic Rocking Vibration of a Rigid Block with Sliding Motion Under Two-Dimensional Harmonic Excitation

**Man-Yong Jeong**
*Department of Electronics & Control Engineering, Numazu College of Technology, Japan*
**Jeong-Ho Kim***
*School of Mechanical and Automotive Engineering, BK21, Sunchon National University, Chonnam 540-742, Korea*
**In-Young Yang**
*School of Mechanical Engineering, Chosun University, Kwangju 501-759, Korea*

This research deals with the influence of nonlinearities associated with impact and sliding upon the rocking behavior of a rigid block, which is subjected to two-dimensional horizontal and vertical excitation. Nonlinearities in the vibration were found to depend strongly on the effect of the impact between the block and the base, which involves an abrupt reduction in the system's kinetic energy. In particular, when sliding occurs, the rocking behavior is substantially changed. Response analysis using a non-dimensional rocking equation was carried out for a variety of excitation levels and excitation frequencies. The chaos responses were observed over a wide response region, particularly, in the cases of high vertical displacement and violent sliding motion, and the chaos characteristics appear in the time histories, Poincare maps, power spectra and Lyapunov exponents of the rocking responses. The complex behavior of chaotic response, in phase space, is illustrated by the Poincare map. The distribution of the rocking response is described by bifurcation diagrams and the effects of sliding motion are examined through the several rocking response examples.

**Key Words:** Rocking Vibration, Rigid Block, Sliding Motion, Poincare Map, Lyapunov

## 1. Introduction

The Hyogoken-nanbu earthquake in January, 1995 carried block objects such as tombstones, historical monuments, refrigerators, furniture, and super computers to tumble over. It was reported as one of the most violent earthquakes for over a century, and produced violent ground motion in the vertical direction. In particular, most collapses and fall over damage incidents reported during the earthquake were caused by violent sliding motion.

Previous studies on this issue were carried out under extremely simplified rocking conditions, which neglected sliding motion (Spanos and Koh, 1984; Tso and Wong, 1989) and the energy dissipation associated with this sliding motion (Aslam et al., 1980; Yim et al., 1980). For most rocking bodies, however, such an ideal condition cannot be assumed. Therefore, it is necessary to investigate the rocking behavior of a rigid body under realistic conditions and to include the nonlinear effects of impact and sliding.

Most experimental work on rocking vibration reported that rocking did not appear although the excitation was periodic (Jeong and Suzuki, 1995). This non-reappearance is caused by non-linearity of the sliding motion of the block and the impact between a block and its base. The

* Corresponding Author,
**E-mail**: kimstime@sunchon.ac.kr
**TEL**: +82-61-750-3963; **FAX**: +82-61-753-3962
School of Mechanical and Automotive Engineering, BK21, Sunchon National University, Chonnam 540-742, Korea. (Manuscript **Received** July 13, 2001; **Revised** June 26, 2002)

contact condition of the block and its base can be delicately changed by altering the block position. Therefore, the rocking response is sensitively influenced by a small change in the contact between the block and its base, and the sliding motion and energy dissipation at that time.

This paper deals with several basic characteristics of the rocking motion as demonstrated by rocking response analysis results using a nonlinear rocking model. The nonlinearities of the rocking system are due to transitions of governing equations and due to energy dissipation during impact between the block and its base.

## 2. Rocking Equations

### 2.1 Rocking equations

Including the sliding motion, the rocking block system subjected to two-dimensional excitation in the horizontal and vertical directions is shown in Fig. 1, where $a_v(t)$ and $a_h(t)$ are the vertical and horizontal excitations, and $x$, $y$ and $\theta$ are the horizontal, vertical and angular displacements of the mass center, respectively. $f_x$ is the reaction force in the horizontal direction and $f_y$ is the reaction force in the vertical direction.

$$a_h > \frac{B}{H}(g + a_v) \tag{1}$$

where $g$ is the gravitational acceleration. The horizontal and vertical reaction forces between the block and the base are given by

$$f_x = ma_h(t) + m\ddot{x} \tag{2}$$

$$f_y = m\ddot{y} + mg + ma_v \tag{3}$$

The condition for sliding during rotation is given by

$$\mu_s \leq \left| \frac{\ddot{x} + a_h}{\ddot{y} + g + a_v} \right| \tag{4}$$

The relationship between the horizontal and vertical reaction forces and the kinetic friction coefficient of sliding or rotational sliding motion is described by

$$\ddot{x} + a_h = -S(\dot{x}_0)\,\mu_k\{\ddot{y} + g + a_v\} \tag{5}$$

The governing equation of motion about the rotation centers $O$ and $O'$ is described by

$$I_o\ddot{\theta} = -(m\ddot{y} + mg + ma_v)R\{S(\theta)\sin(\phi - |\theta|) + S(\dot{x}_0)\,\mu_k\cos(\phi - |\theta|)\} \tag{6}$$

which is defined on the basis of the signum functions, $S(\theta)$ and $S(\dot{x}_0)$. The equations for rocking motion and sliding motion can be expressed as

$$\ddot{\theta} + p^2 f_1(\theta, \dot{\theta}_p, \dot{x}) = 0 \tag{7}$$

$$\ddot{x} + p^2 f_2(\theta, \dot{\theta}_p, \dot{x}) = -a_h(t) \tag{8}$$

where $f_1(\theta, \dot{\theta}_p, \dot{x})$ and $f_2(\theta, \dot{\theta}_p, \dot{x})$ are

$$f_1(\theta, \dot{\theta}_p, \dot{x}) = \frac{S(\theta)\{\sin(\phi - |\theta|) + S(\theta)S(\dot{x}_0)\mu_k\cos(\phi - |\theta|)\}\{1 - \gamma\cos(\phi - |\theta|)\dot{\theta}_p^2\}}{\{1 + \gamma\sin^2(\phi - |\theta|) + \gamma S(\theta)S(\dot{x}_0)\mu_k\cos(\phi - |\theta|)\sin(\phi - |\theta|)\}} \tag{9}$$

$$f_2(\theta, \dot{\theta}_p, \dot{x}) = \frac{\mu_k S(\dot{x}_0)S(\theta)\{1 - \gamma\cos(\phi - |\theta|)\dot{\theta}_p^2\}}{\gamma\{1 + \gamma\sin^2(\phi - |\theta|) + \gamma S(\theta)S(\dot{x}_0)\mu_k\cos(\phi - |\theta|)\sin(\phi - |\theta|)\}} \tag{10}$$

$I_o$ is the moment of inertia about the block edges given by

$$I_o = \frac{4mR^2}{3} \tag{11}$$

The rocking frequency of the block is represented by

$$p^2 = \frac{mgR}{I_0} = \frac{3g}{4R} \tag{12}$$

$$\gamma = \frac{mR^2}{I_o} \tag{13}$$

$$\dot{\theta}_p = \frac{\dot{\theta}}{p} \tag{14}$$

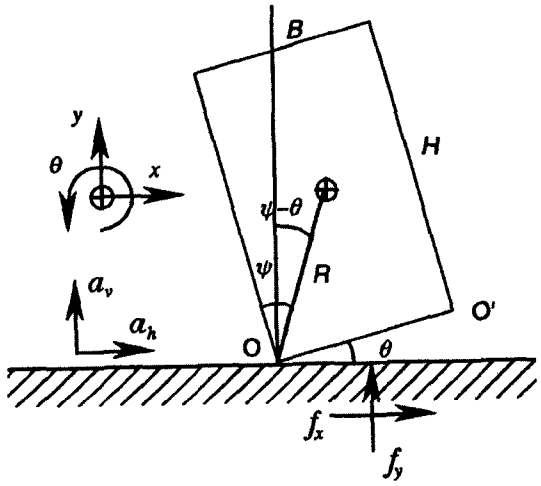


**Fig. 1** Rocking of a rigid block

and the relative horizontal displacement and its velocity are described by

$$x_0=x-S(\theta)R\sin(\psi-|\theta|) \quad (15)$$

$$\dot{x}_0=\dot{x}+R\cos(\psi-|\theta|)\dot{\theta} \quad (16)$$

### 2.2 Impact of block and base

The impact between the block and its base has a large effect on the rocking behavior. Therefore, careful modeling of the impact is essential. The energy related dissipation at impact without sliding motion is constant and depends on the block shape ratio. It is called a coefficient of restitution. However, when sliding occurs, the energy dissipation is affected by the sliding motion and the associated energy loss is largely dependent on the magnitude of the horizontal sliding motion. Using the principle of impulse and momentum, an impact model was established by Shenton (Shenton and Jones, 1991). The effects of the sliding motion on the impact were illustrated in our last study, and therefore, we refer to this paper for a detailed explanation (Jeong and Suzuki, 1997).

In the case of no sliding motion, the post-impact velocity of the mass center, in terms of the scalar components $\dot{x}_2$, $\dot{y}_2$ and $\dot{\theta}_2$, is expressed in terms of the pre-impact velocities $\dot{x}_1$, $\dot{y}_1$ and $\dot{\theta}_1$ as

$$\dot{x}_2=-\frac{H\delta_i}{2}\dot{\theta}_1 \quad (17)$$

$$\dot{y}_2=-S(\theta_1)\frac{B}{2}(\delta_i+2e)\dot{\theta}_1 \quad (18)$$

$$\dot{\theta}_2=\delta_i\dot{\theta}_1 \quad (19)$$

in which the energy dissipation rate is given by

$$\delta_i=1-\frac{3}{4}(1+\lambda_x)\cos^2\psi-\frac{3}{2}(1+e)\sin^2\psi \quad (20)$$

where the rate of change in the horizontal and angular velocities $\lambda_x$ and the restitution coefficient $e$ are defined by

$$\lambda_x=\frac{2\dot{x}_1}{H\dot{\theta}_1} \quad (21)$$

$$e=1-\frac{3}{2}\sin^2\psi \quad (22)$$

If sliding does not occur, the rate of change in the horizontal and angular velocities $\lambda_x$ will be $-1$. The sliding occurrence condition at impact is expressed by

$$\bar{\mu}_s\geq\frac{H}{B}\left|\frac{\delta_i+\lambda_x}{1+2e+\delta_i}\right| \quad (23)$$

and the relationship between pre-impact and post-impact velocities becomes

$$\dot{x}_2=\dot{x}_1+S(\theta_1)S(\dot{x}_{i2})\bar{\mu}_k\frac{B}{2}(1+\bar{\delta}_i+2e)\dot{\theta}_1 \quad (24)$$

$$\dot{y}_2=-S(\theta_1)\frac{B}{2}(\bar{\delta}_i+2e)\dot{\theta}_1 \quad (25)$$

$$\dot{\theta}_2=\delta_i\dot{\theta}_1 \quad (26)$$

in which the energy dissipation rate is expressed as

$$\bar{\delta}_i=\frac{1-3\left(1-S(\theta_1)S(\dot{x}_{i2})\bar{\mu}_k\frac{H}{B}\right)(1+2e)\sin^2\psi}{1+3\left(1-S(\theta_1)S(\dot{x}_{i2})\bar{\mu}_k\frac{H}{B}\right)\sin^2\psi} \quad (27)$$

## 3. Rocking Response Analysis

The rocking period of a block depends on the block size parameter $R$ as shown in Eq. (7). Therefore, the rocking frequency $p$ is the most significant parameter in the rocking system. The rocking equation is normalized by setting $\Theta=\theta/\Psi$, $p_t=\tau$, $\Omega=\omega$, $X=x/R$ and $X_o=x_o/R$ to simplify the problem. As a result, the normalized rocking equations are expressed by

$$\ddot{\Theta}+p^2f_1(\Theta,\dot{\Theta}_p,\dot{X})=0 \quad (28)$$

$$\ddot{X}+p^2f_2(\Theta,\dot{\Theta}_p,\dot{X})=-\frac{a_h(t)}{R} \quad (29)$$

$$f_1(\Theta,\dot{\Theta}_p,\dot{X})=\frac{S(\theta)\{\sin\phi(1-|\theta|)+S(\theta)S(\dot{X}_o)\mu_k\cos\phi(1-|\theta|)\}\left\{1+\frac{a_v}{g}-\gamma\cos\phi(1-|\theta|)\dot{\theta}^2\right\}}{\{1+\gamma\sin^2\phi(1-|\theta|)+\gamma S(\theta)S(\dot{X}_o)\mu_k\cos\phi(1-|\theta|)\sin\phi(1-|\theta|)\}} \quad (30)$$

$$f_2(\Theta,\dot{\Theta}_p,\dot{X})=\frac{\mu_k S(\theta)S(\dot{X}_o)\left\{1+\frac{a_v}{g}-\gamma\cos\phi(1-|\theta|)\dot{\theta}^2\right\}}{\gamma\{1+\gamma\sin^2\phi(1-|\theta|)+\gamma S(\theta)S(\dot{X}_o)\mu_k\cos\phi(1-|\theta|)\sin\phi(1-|\theta|)\}} \quad (31)$$

The normalized horizontal displacement $X_o$ of the block edge is expressed in terms of the normalized mass center displacement $X$ and the normalized angular displacement $\Theta$.

$$X_o=X-S(\Theta)\sin\psi(1-|\Theta|) \quad (32)$$

$$\dot{X}_o=\dot{X}+\cos\psi(1-|\Theta|)\dot{\Theta} \quad (33)$$

In this study, the horizontal and vertical base excitations are assumed to be described by

$$a_h(t)=A_h\psi g\sin(\Omega\tau+\Phi) \tag{34}$$

$$a_v(t)=A_v\psi g\sin(\Omega\tau+\Phi) \tag{35}$$

When the block is rotating without sliding, the normalized post-impact velocities are expressed by

$$\dot{X}_2=-\frac{H\psi\delta_i}{2R}\dot{\Theta}_1 \tag{36}$$

$$\dot{Y}_2=-S(\Theta_1)\frac{B\psi}{2R}(\bar{\delta}_i+2e)\dot{\Theta}_1 \tag{37}$$

$$\dot{\Theta}_2=\delta_i\dot{\Theta}_1 \tag{38}$$

in which

$$\lambda_x=\frac{2\dot{X}_1}{H\dot{\Theta}_1} \tag{39}$$

and the normalized energy dissipation rate is the same as that shown in Eq. (20). When the block is rotating and sliding, the normalized post-impact velocities are expressed by

$$\dot{X}_2=\dot{X}_1+S(\Theta_1)S(\dot{X}_{i2})\bar{\mu}_k\frac{B\psi}{2R}(1+\bar{\delta}_i+2e)\dot{\Theta}_1 \tag{40}$$

$$\dot{Y}_2=-S(\Theta_1)\frac{B\psi}{2R}(\bar{\delta}_i+2e)\dot{\Theta}_1 \tag{41}$$

$$\dot{\Theta}_2=\delta_i\dot{\Theta}_1 \tag{42}$$

Then, the normalized energy dissipation becomes

$$\bar{\delta}_i=\frac{1-3\left\{1-S(\Theta_1)S(\dot{X}_{i2})\bar{\mu}_k\frac{H}{B}\right\}(1+2e)\sin^2\psi}{1+3\left\{1-S(\Theta_1)S(\dot{X}_{i2})\bar{\mu}_k\frac{H}{B}\right\}\sin^2\psi} \tag{43}$$

Using the Ralston's Runge-Kutta method, rocking response analysis was carried out in order to investigate the chaotic characteristics of a rocking system. The normalized sampling time of numerical integration 0.004 and is decreased by a factor of ten in the part of signum change until normalized angular displacement becomes sufficiently small, namely, under $10^{-6}$. The transition of the rocking equation is carried out using Eq. (8) for the kinetic energy dissipation at impact. The algorithm of the rocking response analysis program is shown in Fig. 2 and this was further developed in order to obtain accurate results on numerical analysis. The algorithm includes the two processes of rotation and impact; i.e., the rotational

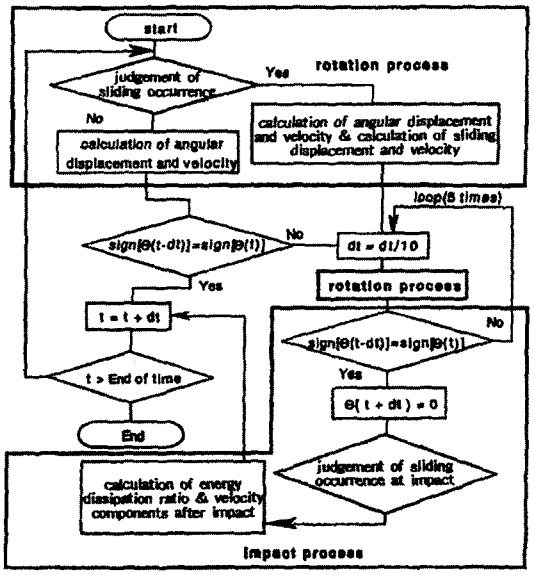


**Fig. 2** Algorithm of the rocking response analysis program

process judges sliding as a rotational motion, by Eq. (4) and solves the simultaneous Eqs. (30) and (31) by the Ralston's Runge-Kutta method. The impact process determines the point of normalized angular displacement 0 approximately, and calculates the post-impact velocity using Eq. (20) or (27) and then exchanges the signum function $S(\Theta)$ in the rocking equation.

## 4. Examination of Rocking Response

In order to investigate the nonlinear characteristics of a rocking system with sliding motion, rocking responses *without sliding were first examined*. The effect of sliding motion upon the rocking behavior was examined by comparing no-sliding-rocking with sliding-and-rocking.

The rocking response characteristics were examined by comparing the no sliding case with the sliding case for different distributions of rocking mode and trajectories in phase space. The chaotic behavior is characterized by a random-like, unpredictable aspect as well as a rocking motion, although the excitation is deterministic and periodic. Unpredictability arises from the extremely sensitive dependence of rocking response on initial conditions, and system and excitation para-

meters. Nearly identical trajectories of chaotic motion, with seemingly infinitesimally different initial conditions, diverge exponentially, leading to large differences in the long-term predictions of the response. In this study, the next four methods are used in the response analysis to examine rocking responses.

Bifurcation diagrams show changes in system characteristics for given changes in system or excitation parameters. The bifurcation diagram is a plot of the normalized angular displacement against the excitation force 0 in the rocking response data from 150,000 to 200,000. Therefore, the diagram corresponds to Poincare's point for the zero excitation force. The Poincare map is constructed from strobe points in the phase space of the rocking response associated with an zero excitation force. It appears as a strange attractor in the case of chaotic response, and as one or more fixed points in the case of periodic response. The spectral density function is also useful for examining the periodicity of response. Periodic, quasi-periodic, and chaotic responses have a single dominant frequency, a finite number of incommensurate frequencies, and an infinite number of frequencies (i.e., a wideband spectrum), respectively. Power spectra of rocking response are created by using a time history of from 3,000 to 7,096. The Lyapunov exponent is a quantitative measure of the divergence rate of trajectories in phase space. The Lyapunov exponent of chaotic response is positive, whereas those of the quasi-periodic and periodic responses are zero and minus, respectively.

### 4.1 Rocking response without sliding

To investigate dependence of rocking responses upon excitation amplitude, numerical analysis was carried out when the other parameters were fixed. The fixed system and excitation parameters were, $B=1$ m, $H=4$ m, $e=0.925$ and $\Omega_h=8$ or 10, the excitation amplitude in the vertical direction was the only variable, which was examined from 0 to 3, in the rocking response analysis and the excitation frequencies were limited to the same values in the horizontal and vertical directions. The bifurcation diagram was formed for the sampling amplitude of 0.02 and the blank in the diagram means the tumbling of the block. Figs. 3~4 show the bifurcation diagrams of the rocking responses for $\Omega_h=\Omega_v=8$, $A_v=0\sim3$ and $A_h=3$, respectively.

Figs. 5~6 are the bifurcation diagrams obtained with the same conditions except for $\Omega_h=\Omega_v=10$. As shown in these bifurcation diagrams, there are three types of rocking responses, namely, stable periodic rocking responses, chaotic rocking responses and tumble responses. Firstly, Fig. 3 shows the periodic response of the (1,1) mode from 0 to about 0.7, of vertical amplitude. Periodic responses of the (1,2) mode from about 0.7 to 1.25 and the higher order rocking periodic and chaotic responses coexist in the region over the normalized vertical amplitude of 1.25. On the other hand, Fig. 4 shows the periodic response of

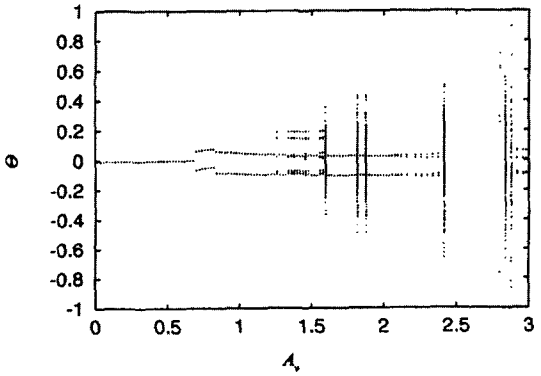


**Fig. 3** Bifurcation diagram for rocking responses ($\Omega_h=\Omega_v=8$, $A_h=2.0$, $A_v=0\sim3$)

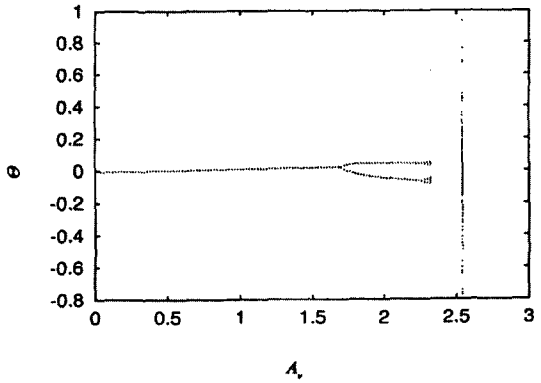


**Fig. 4** Bifurcation diagram for rocking responses ($\Omega_h=\Omega_v=8$, $A_h=3.0$, $A_v=0\sim3$)

the (1,1) mode, in the rocking response region, from 0 to about a vertical amplitude 1.7, and the periodic response of the (1,2) mode from about 1.7 to 2.25, and the periodic response of the (1,4) mode from about 2.25 to 2.3 and a chaotic response after 2.3. Figs. 5~6 show the same tendency as Figs. 3~4, but the region of the periodic response is wider and the region of tumbling narrower. In the case of Fig. 4 and Fig. 6, the diagrams apparently show a periodic-double bifurcation for a change of vertical amplitude, but the two diagrams of Figs. 3 and 5 show intermittency bifurcation. When comparing equal amplitudes, it follows that the region of periodic and quasi-periodic responses is expanded with increase in the excitation frequency, the chaotic region narrows and the tumbling response decreases.

Examples of chaotic responses in the bifurcation diagram of Figs. 3 and 6 are shown in Figs. 7~8, in which figures (a), (b) and (c) indicate the time history, the power spectra and the

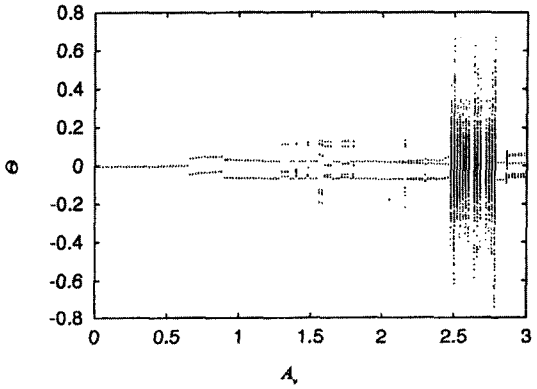


**Fig. 5** Bifurcation diagram for rocking responses ($\Omega_h=\Omega_v=10$, $A_h=2.0$, $A_v=0\sim3$)

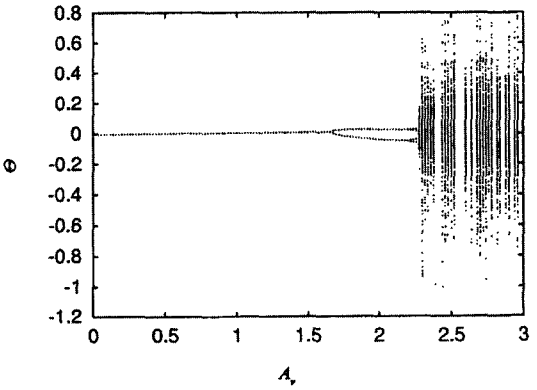


**Fig. 6** Bifurcation diagram for rocking responses ($\Omega_h=\Omega_v=10$, $A_h=3.0$, $A_v=0\sim3$)

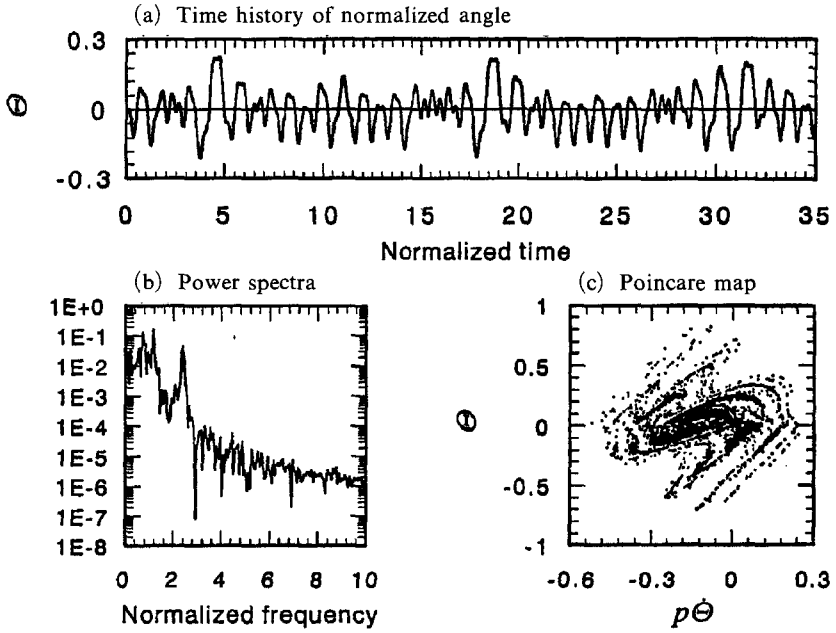


**Fig. 7** Rocking response without sliding ($\Omega_h=\Omega_v=8$, $A_h=2.0$, $A_v=2.5$)

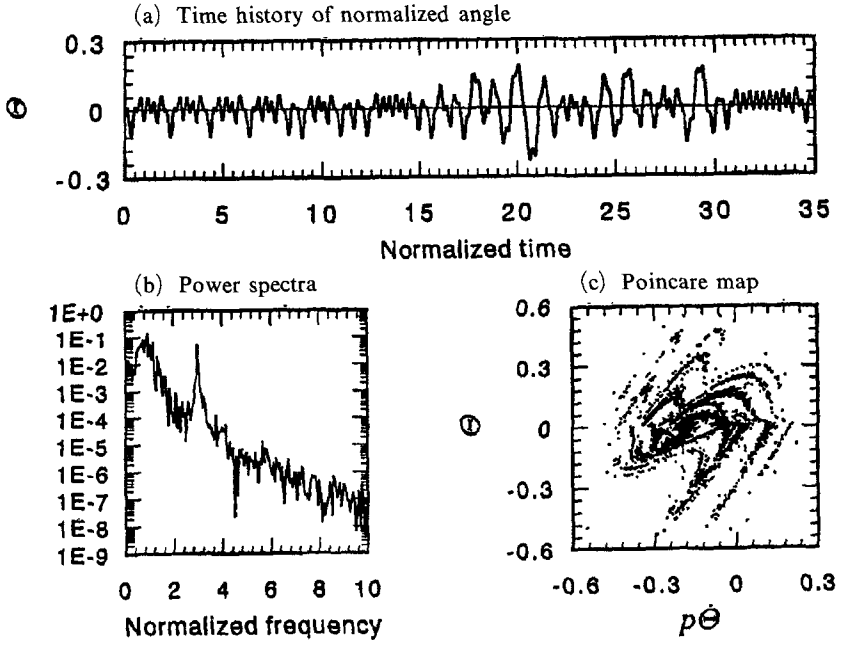


**Fig. 8** Rocking response without sliding ($\Omega_h=\Omega_v=10$, $A_h=3.0$, $A_v=2.5$)

Poincare map for the rocking response, respectively. The maximum amplitude of the rocking response when $\Omega_h=\Omega_v=8$ is larger than for $\Omega_h=\Omega_v=10$ although the excitation amplitude in the horizontal direction $A_h$ is smaller. These figures illustrate that responses at lower input frequencies are expanded widely in the phase space and that the chaotic attractor is composed of multiple limit cycles, which are characterized by a unique shape, which is 'asymmetrical' to zero angular displacement and 'whirled' in the counter clockwise direction. The Lyapunov exponents for these chaotic responses were 0.74 and 1.02, respectively.

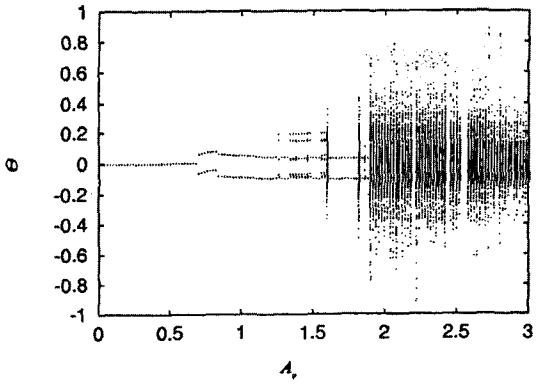


**Fig. 9** Bifurcation diagram for rocking responses ($\Omega_h=\Omega_v=8$, $A_h=2.0$, $A_v=0\sim3$, $\mu_s=\bar{\mu}_s=0.4$, $\mu_k=\bar{\mu}_k=0.35$)

### 4.2 Rocking response with sliding

In this section, in order to investigate the effect of sliding motion upon rocking response, we compared the rocking with the rocking-with-sliding responses. The bifurcation diagram for rocking response with $\Omega_h=\Omega_v=8$, $A_v=0\sim3$, and $A_h=2$, and a static friction coefficient, $\mu_s=\bar{\mu}_s=0.4$ and a kinetic friction coefficient, $\mu_k=\bar{\mu}_k=0.35$ as shown in Fig. 9. The bifurcation diagram for the same conditions, except $\mu_s=\bar{\mu}_s=0.35$ and $\mu_k=\bar{\mu}_k=0.3$, is shown in Fig. 10. The upper bar means the frictional coefficient at impact. The rocking behavior is affected by the sliding motion in the horizontal direction, and the distribution of the rocking response is dependent on the frictional coefficient. An example is shown in Fig. 10, in this case, the Lyapunov exponent was 0.51.

We next examinded the two rocking responses to investigate the effect of sliding on rocking

response, which shows chaotic behavior even without sliding. Figure 11 shows an example for $\Omega_h=\Omega_v=8$, $A_h=2$, and $A_v=2.0$, the static friction coefficient and the kinetic friction coefficient. Figures. 7, 12~13 show responses for the identical excitation condition, but with a different frictional coefficient, the attractor shape becomes smaller on lowering the frictional coefficient, and it is shown that the maximum amplitude of the rocking response is lowered. Though it had reached a tumbling level in the case of Fig. 6, the maximum amplitude was about 0.75 in Fig. 12, and this became about 0.4 in Fig. 13. Lowering of the frictional force between the block and the base, and this increasing energy dissipation by sliding, produced a smaller rocking response attractor shape and a smaller rocking response maximum amplitude, if the excitation frequencies in the horizontal and vertical directions are identical. The Lyapunov exponents for the rocking response of Figs. 12~13 were 0.71 and 1.34, respectively.

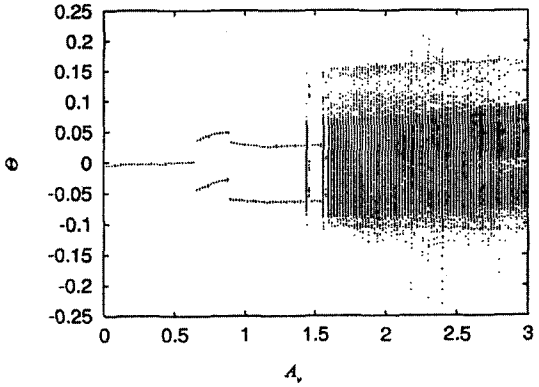


**Fig. 10** Bifurcation diagram for rocking responses ($\Omega_h=\Omega_v=8$, $A_h=2.0$, $A_v=0\sim3$, $\mu_s=\bar{\mu}_s=0.35$, $\mu_k=\bar{\mu}_k=0.3$)

The bifurcation diagram for rocking responses with $\Omega_h=\Omega_v=10$, $A_v=0\sim3$, $A_h=3$, is shown in Fig. 14. The bifurcation diagram for the same conditions used in Fig. 14 is shown in Fig. 15. The chaotic response region is expanded in these bifurcation diagrams by lowering its frictional coefficient. The examples of rocking response in

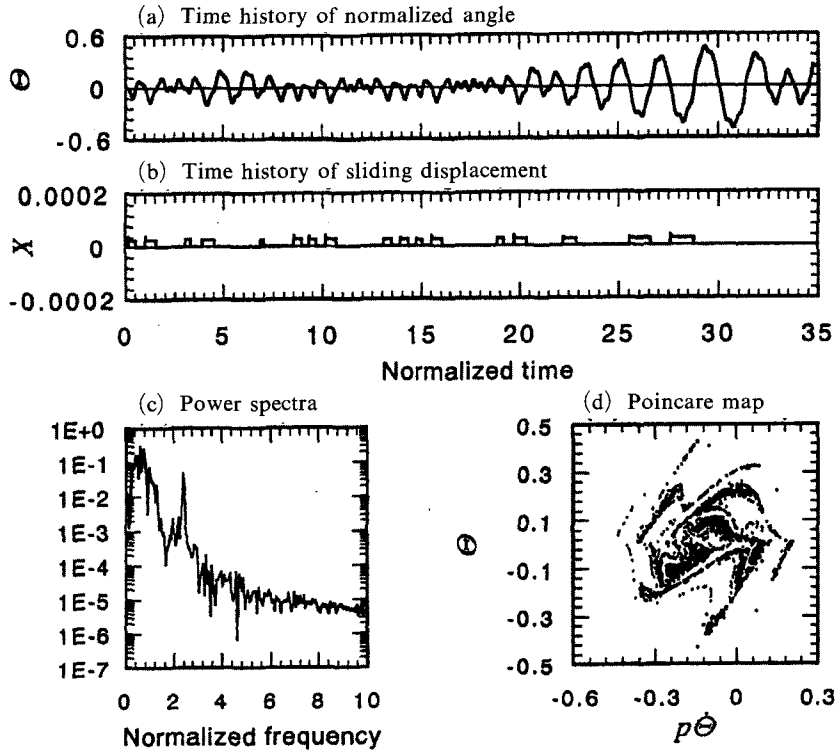


**Fig. 11** Rocking response with sliding ($\Omega_h=\Omega_v=8$, $A_h=2.0$, $A_v=2.0$, $\mu_s=\bar{\mu}_s=0.4$, $\mu_k=\bar{\mu}_k=0.35$)

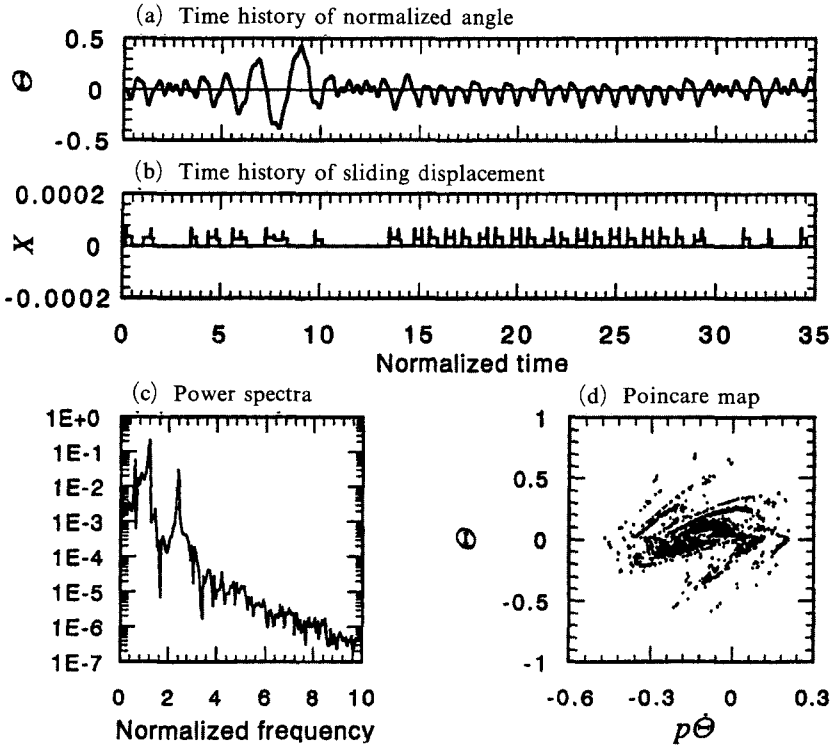


**Fig. 12** Rocking response with sliding ($\Omega_h=\Omega_v=8$, $A_h=2.0$, $A_v=2.5$, $\mu_s=\bar{\mu}_s=0.4$, $\mu_k=\bar{\mu}_k=0.35$)

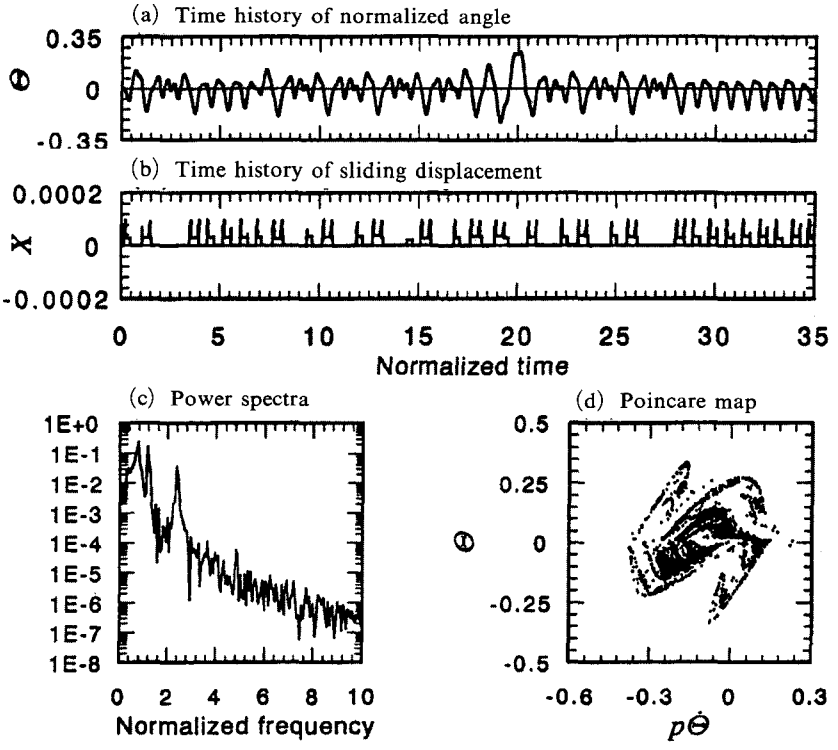


**Fig. 13** Rocking response with sliding ($\Omega_h=\Omega_v=8$, $A_h=2.0$, $A_v=2.5$, $\mu_s=\bar{\mu}_s=0.35$, $\mu_k=\bar{\mu}_k=0.3$)

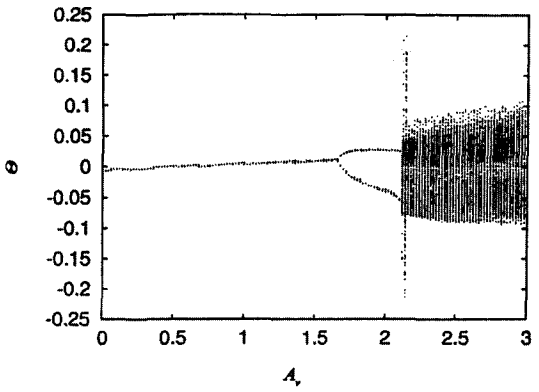


**Fig. 14** Bifurcation diagram for rocking responses ($\Omega_h=\Omega_v=10$, $A_h=3.0$, $A_v=0\sim3$, $\mu_s=\bar{\mu}_s=0.4$, $\mu_k=\bar{\mu}_k=0.35$)

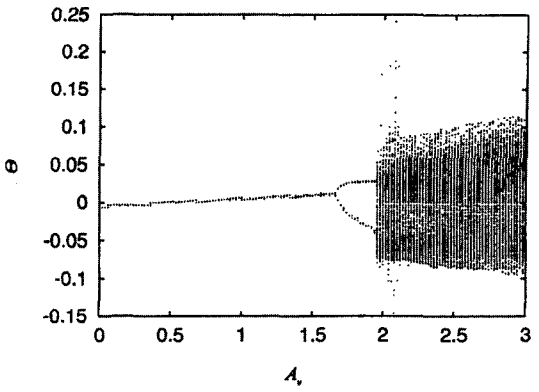


**Fig. 15** Bifurcation diagram for rocking responses ($\Omega_h=\Omega_v=10$, $A_h=3.0$, $A_v=0\sim3$, $\mu_s=\bar{\mu}_s=0.35$, $\mu_k=\bar{\mu}_k=0.3$)

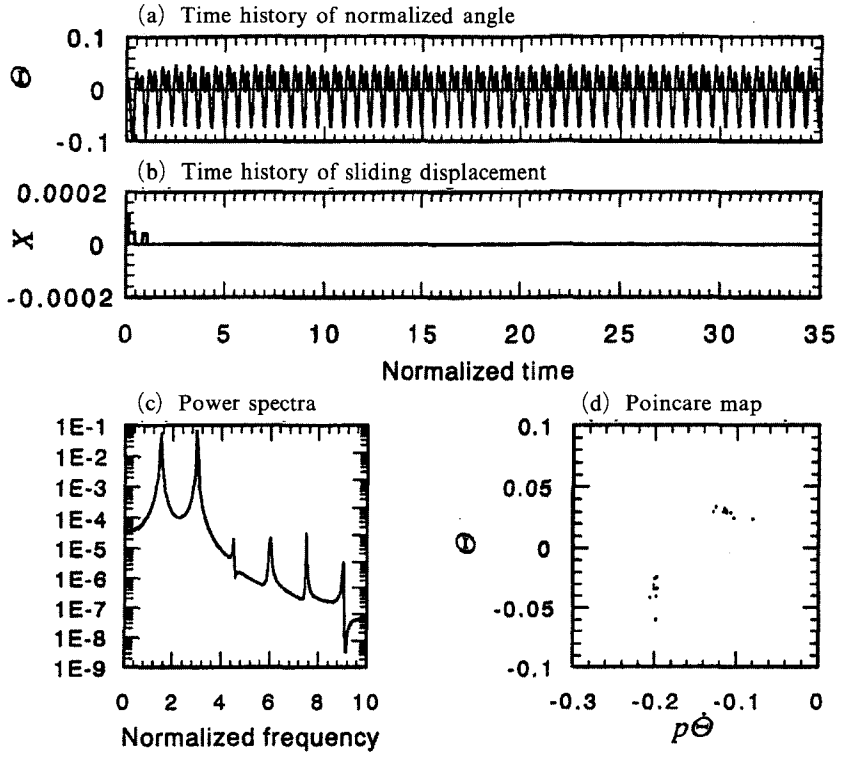


**Fig. 16** Rocking response (with sliding) ($\Omega_h=\Omega_v=10$, $A_h=3.0$, $A_v=2.0$, $\mu_s=\bar{\mu}_s=0.4$, $\mu_k=\bar{\mu}_k=0.35$)

Fig. 14 are shown in Figs. 16~17. By comparing the bifurcation diagrams shown in Figs. 9~10, it may be understood that the chaotic response region is widely extended at higher excitation frequencies and becomes wider in the case with sliding than in the case without sliding. That is, the frictional force between the block and its base affects the rocking response at higher excitation frequencies, and the sliding movement is also intense.

### 4.3 Sliding and the attractor shape

In this section, we examine the influence of sliding upon attractor shape. When the horizontal

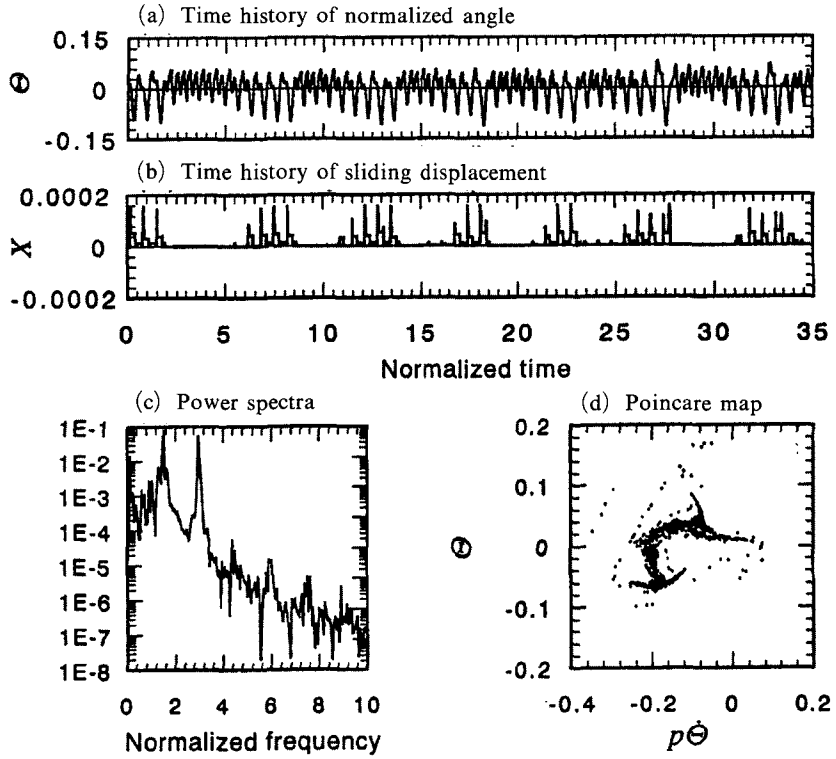


**Fig. 17** Rocking response with sliding ($\Omega_h=\Omega_v=10$, $A_h=3.0$, $A_v=2.0$, $\mu_s=\bar{\mu}_s=3.35$, $\mu_k=\bar{\mu}_k=0.3$)

excitation amplitude is comparatively small, as shown in Figs. 7, 12~13, the number of attraction regions decreases on lowering the friction coefficient, and the attractor becomes more compact in shape, and the fundamental form of the attractor does not change. However, when the excitation amplitude is comparatively large at $A_h=3$, the shape of the attractor is comparable to the case without sliding, as shown in Figs. 18~19. This means that the magnitude of horizontal displacement by sliding produces large effects in the shape of the attractor. The change in the shape of the attractor increases as the sliding motion is increased, and when the horizontal displacement produced by sliding is large, and it takes a form which inclines toward the negative direction for the rotational velocity axis. The Lyapunov exponents for these responses were 1.91 and 1.76. Lyapunov exponent increases more so in the presence of sliding. It follows that the sliding motion intensifies the chaoticity of the rocking response. In the case of the rocking vibration created by the two-dimensional input in which the horizontal and vertical excitation frequencies are identical, sliding occurs only in the reverse direction of the rocking, because it is fixed by the excitation amplitude and frequency in the horizontal and vertical directions, the vibration direction of the base is fixed in some direction, and the reverse-directioned rotational displacement with sliding induced by rocking also increases. For rocking vibration with sliding, it becomes the unstable motion in which only the other rotational displacement by the effect of sliding motion increases, as described previously. It is estimated that the effect on rocking response increases, if any disturbance is applied to this exercise condition for the rocking vibration system. That is, the oscillation which cannot be simply considered in the analytical model seems to exist on the lowering cause of the tumble condition and the non-reappearance of the experimental rocking response with sliding in research to date. Minute changes in the frictional force and the contact between the block and the base occur as a result of considering this oscillation. It

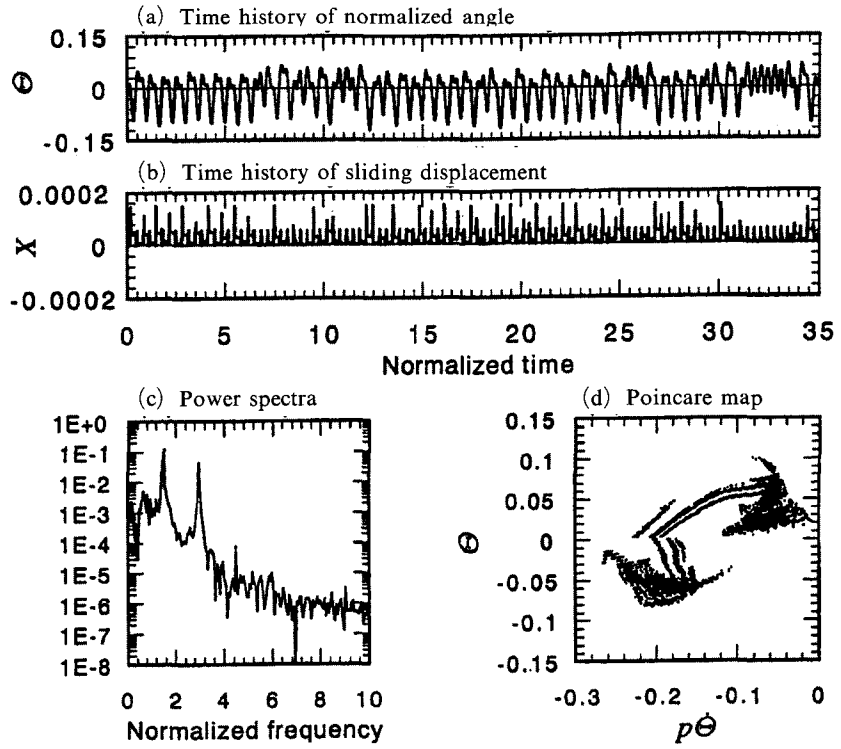


**Fig. 18** Rocking response with sliding ($\Omega_h=\Omega_v=10$, $A_h=2.5$, $A_v=2.0$, $\mu_s=\bar{\mu}_s=0.4$, $\mu_k=\bar{\mu}_k=0.35$)

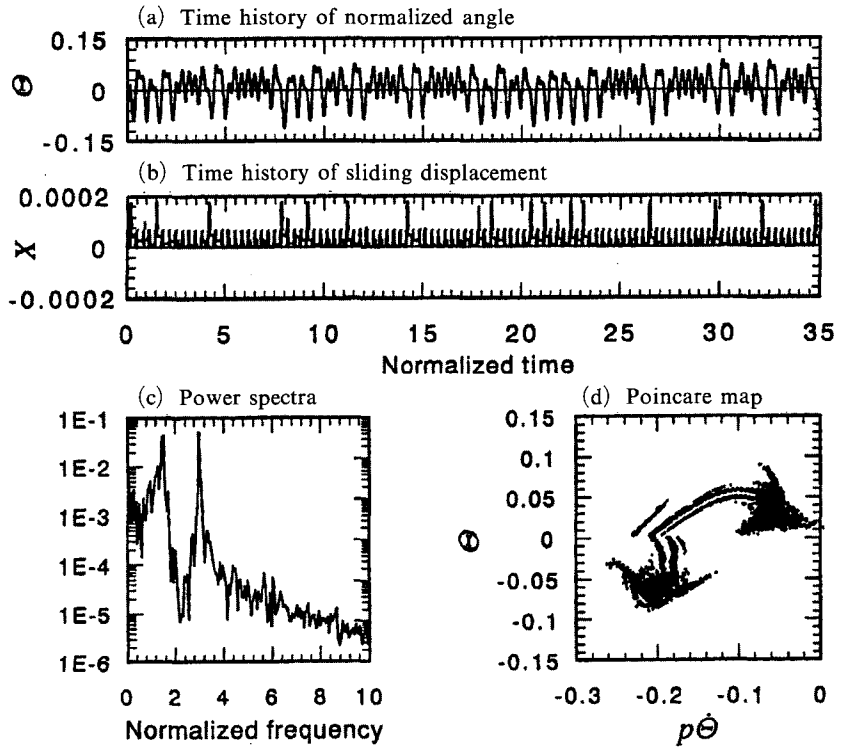


**Fig. 19** Rocking response with sliding ($\Omega_h=\Omega_v=10$, $A_h=3.0$, $A_v=2.5$, $\mu_s=\bar{\mu}_s=0.35$, $\mu_k=\bar{\mu}_k=0.3$)

cannot be said that the rocking vibrational characteristics caused by the two-dimensional excitation were sufficiently able to be grasped, since in this paper, it forced the excitation frequency to be 8 and 10, and limited, when the normalized excitation frequency in the horizontal direction was identical to that in the vertical direction.

In particular, we intend examining rocking vibration in which the excitation frequency in the horizontal direction differs from that in the vertical direction in the future. Moreover, it is necessary from the chaotic dynamic viewpoint that consideration of the experimental rocking vibration response is more exactly carried out to clarify these nonlinearities of impact and provide more precise rocking behavior characteristics, because it seems to account for minute fluctuations of frictional force between the block and base and the energy dissipation at the time of impact in a real rocking vibration system.

## 5. Conclusions

(1) In the case of no sliding, the regions of periodic and quasi-periodic responses are expanded with an increase in the excitation fre quency, the chaotic region narrows and the tumbling response decreases. The intermittency chaos, in which the periodic response intermingles with the chaotic response for a comparatively small level change in excitation amplitude is shown, and at high excitation amplitude, it changes to chaotic response by period-doubling.

(2) There is a case in which it becomes a chaotic response by sliding, even in the region showing a periodic response in the case of no sliding. That is, the chaotic response region gets wider when sliding occurs.

(3) When sliding occurs, the size of an attractor prevented by a rocking response caused by lowering the friction force between the block and the base decreases, and the maximum amplitude of the rocking response also decreases. The periodic response region narrows with the lowering of the frictional force and the chaotic response region is expanded.

(4) The magnitude of the horizontal displacement carried by sliding has an influence on the attractor shape of the rocking response. Moreover, the shape of the attractor reduces and the attractor becomes biased in a negative direction for the angular velocity axis. In this case, the Lyapunov exponent increases and chaoticity of the rocking response is strengthened.

## Acknowledgment

This study was supported by research funds from Chosun University, 2001.

## References

Aslam, M., Godden, W. G. and Scalise, D. T., 1980, "Earthquake Rocking Response of Rigid Bodies," *Journal of Engineering Structure, ASCE*, 106(2), pp. 377~392.

Jeong, M. Y. and Suzuki, K., 1995, "A Basic Study on the Dynamic Behavior of Rocking Rigid Body Structure," *Asia-Pacific Vibration Conference '95*, 95-1, pp. 365~370.

Jeong, M. Y. and Suzuki, K., 1997, "Experimental Investigation of Rocking Vibration Characteristics by two Dimensional Excitation," *The 74th JSME Spring Annual Meeting*, 74(4), pp. 124~127.

Jeong, M. Y. and Suzuki, K., 1997, "A Study on the Dynamic Behavior of Rocking Rigid Body Using Nonlinear Rocking Model," *Pressure Vessels & Piping Division Conference '97*, 97-4, pp. 27~34.

Lin, H. and Yim, S. C. S., 1996, "Nonlinear Rocking Motions Overturning Under Random Excitations. I," *Journal of Engineering Mechanics, ASCE*, 122(8), pp. 719~727.

Lin, H. and Yim, S. C. S., 1996, "Nonlinear Rocking Motions Overturning Under Random Excitations. II," *Journal of Engineering Mechanics, ASCE*, 122(8), pp. 728~735.

Shenton, H. W. and Jones, N. P., 1991, "Base Excitation of Rigid Bodies : ForMulation," *Journal of Engineering Mechanics*, Vol. 117, No. 10, pp. 2286~2306.

Solomon, C. S. Yim and Huan Lin, 1991,

"Nonlinear Impact and Chaotic Response of Slender Rocking Objects," *Journal of Engineering Mechanics*, Vol. 117, No. 9, pp. 2079~2100.

Spanos, P. D. and Koh, A. S., 1984, "Rocking of Rigid Blocks Due to Harmonic Shaking," *Journal of Engineering Mechanics Div.*, ASCE, Vol. 110, No. 11, pp. 1627~1642.

Tso, W. K. and Wong, C. M., 1989, "Steady State Rocking Response Od Rigid Blocks Part I : Analysis," Earthquake Engineering Structure Dynamics, 18(106), pp. 89~106.

Yim, C. S., Chopra, A. K. and Penzien, J., 1980, "Rocking Response of Rigid Blocks to Earthquakes," *Earthquake Engineering Structure Dynamics*, Vol. 8, No. 6, pp. 565~587.